LOW NOISE MEASUREMENT OF PHOTOCURRENT FOR CONTINUOUS GLUCOSE MONITORING

Low Noise Measurement System Enables Continuous Monitoring of Glucose in Subcutaneous Interstitial Fluid

Daniel W. Cooley[1] and David R. Andersen[1,2]
[1]*Department of Electrical and Computer Engineering, The University of Iowa, 132 IATL, Iowa City, IA, U.S.A.*
[2]*Department of Physics, The University of Iowa, 132 IATL, Iowa City, IA, U.S.A.*

Keywords: Continuous glucose monitoring, IR photodiode, Transimpedance amplifier.

Abstract: We have developed a data acquisition unit (DAU) for continuous, low noise measurement of glucose concentration in subcutaneous interstitial fluid (ISF). The system is comprised of a glucose sensor (Olesberg, 2006), op-amps for signal conditioning, and delta-sigma (Δ-Σ) ADCs. The glucose sensor has two IR LEDs which emit light with wavelength of 2.2 to 2.4 μm where there are peaks in the glucose absorption spectrum. The IR light propagates through a glass fluid chamber containing interstitial fluid and a linearly variable bandpass filter before impinging on a 32 channel photodiode array. The center frequency of the filter varies along one dimension of the filter, so that each photodiode is sensitive to equally spaced portions of the glucose absorption spectrum. Transimpedance amplifiers (TIAs) convert the photocurrents into voltages which are sampled by ADCs. We developed a noise model which predicts the noise characteristics of the system. We use low noise metal film resistors to verify the DAU noise characteristics. Non-ideal characteristics such as limited photocurrent and low photodiode shunt resistance increase difficulty of obtaining low noise measurements. We demonstrate that the DAU provides low noise (41.7 dB SNR) photocurrent measurements and is suitable for use in a continuous glucose monitoring system.

1 INTRODUCTION

We have designed and demonstrated a data acquisition unit for low noise measurement of glucose in subcutaneous ISF. In the future the glucose sensor and DAU will be miniaturized for use in an implantable, continuous glucose monitor. The motivation for this research is clear as 23.8 million people in the U.S.A. had diabetes as of 2007 (CDC, 2007). Self monitoring of blood glucose (SMBG) is one important method used to control diabetes (Saudek, 2006)(Chia, 2004). Efforts towards continuous monitoring of blood glucose are under way to prevent high and low blood sugar conditions and to use as part of an artificial pancreas offering a type of "cure" for diabetes (Chia, 2004). We measure the glucose concentration in ISF instead of whole blood because it provides several advantages. Measuring ISF glucose by an implanted device is less painful and less invasive than repeated use of finger-sticks to measure blood glucose concentration (Rebrin, 2000). An implantable glucose monitor would also require limited user intervention and not require the cost of materials required for SMBG with finger-sticks (Olesberg, 2006).

The glucose sensor measures the absorption spectrum of glucose by passing IR light through a fluid chamber containing ISF to a spectrometer. Two LEDs provide IR light with wavelength in the range 2.2 to 2.4 um, near features of the glucose absorption spectrum. The light propagates through a linearly variable bandpass filter before impinging on a 32 element photodiode array. Measuring the current from each photodiode provides data for determining the spectrum of the analyte. Our IR photodiodes have low photocurrent due to the limited amount of light that reaches the filter and is transmitted to each photodiode. This limits the maximum SNR the system can achieve. The shunt resistance, R_T, of the photodiodes is relatively low which also limits the system SNR. The DAU must provide low noise glucose measurements at a

W. Cooley D. and R. Andersen D. (2010).
LOW NOISE MEASUREMENT OF PHOTOCURRENT FOR CONTINUOUS GLUCOSE MONITORING - Low Noise Measurement System Enables Continuous Monitoring of Glucose in Subcutaneous Interstitial Fluid.
In *Proceedings of the Third International Conference on Biomedical Electronics and Devices*, pages 195-200
DOI: 10.5220/0002747901950200

frequency of 1 Hz on a continuous basis. We use low noise metal film resistors to simulate the glucose sensor while evaluating noise characteristics of the DAU.

2 THEORY

2.1 Glucose Sensor

Figure 1 shows a schematic of the glucose sensor. The sensor has two IR LEDs. LED1 emits light directly into the fluid chamber containing ISF and through the linearly variable filter to the 32 channel photodiode array. Light from LED2 goes around the fluid chamber before reaching the filter and photodiodes. The fluid chamber is a thin-walled capillary with square cross section and 0.8 mm inner dimensions. The center frequency of the linearly variable bandpass filter changes along the length of the filter within the 2.2 to 2.4 μm wavelength range. Thus each photodiode collects light from a different portion of the glucose absorption spectrum when LED1 is on. As IR light from LED1 propagates through the ISF sample, glucose absorbs a portion of the light near peaks in the glucose absorption spectrum.

When the glucose sensor is used with the DAU, we measure photocurrents with one LED on at a time and also without any LEDs on in order to normalize and compensate the sensor data for temperature changes. To verify the DAU noise characteristics in preparation for use with glucose sensors we use low noise metal film resistors with resistance equal to the photodiode shunt resistance in place of the photodiodes.

Next we develop a mathematical model for the noise present in the DAU to evaluate the system noise performance.

2.2 Noise Model

2.2.1 Transimpedance Amplifier

Two types of noise that affect the system operation are thermal noise and shot noise (Motchenbacher, 1993). The random motion of charge carriers in a conductor causes thermal noise, also known as Johnson noise. The thermal noise voltage of a resistor R is in series with the resistor and is

$$E_T = \sqrt{4kTR\Delta f}\ , \qquad (1)$$

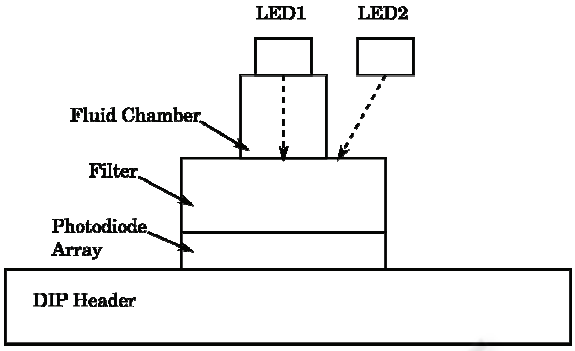

Figure1: The glucose sensor. LED1 emits light through fluid chamber to the filter and diode array. LED2 light goes around the fluid chamber.

where k is Boltzmann's constant, T is temperature in Kelvin, and Δf is the measurement bandwidth. The series combination of the resistor and its thermal noise voltage may be converted into a current source of value E_T/R in parallel with the resistor. Shot noise occurs in transistors and diodes and is due to quantized current flowing across a potential barrier. The shot noise current for I amps of current is

$$I_S = \sqrt{2qI\Delta f}\ , \qquad (2)$$

where q is the electronic charge.

We chose the transimpedance amplifier, Figure 2, to convert photodiode current into a voltage for measurement by an ADC. Another method would be to use a current input ADC, but we chose the TIA in order to maximize the system SNR. To develop the noise model we start with a schematic for the TIA including op amp noise terms (Steffes, 2005) as shown in Figure 3. Here E_{NI} is the op amp input noise voltage, I_{BI} is the op amp input current noise, R_T is the test resistor simulating the photodiode shunt resistance, I_{RT} is the noise current equivalent to the thermal noise from R_T, R_F is the feedback resistor, and E_{RT} is the feedback resistor thermal noise. We omitted the photodiode series resistance from the noise model because of its relatively small magnitude.

We find an expression for the noise at the TIA output by incoherently adding the noise terms (E_{NI}, I_{BI}, I_{RT}, and E_{RF}) multiplied by the gain between the noise term and the TIA output. With $G_N = 1 + R_F/R_T$ and combining some terms, the noise voltage at the TIA output is Eq. 2 from (Steffes, 2005) with $R_S = 0$:

$$E_O = \sqrt{(E_{NI}G_N)^2 + (I_{BI}R_F)^2 + 4kTR_FG_N}\ . \qquad (3)$$

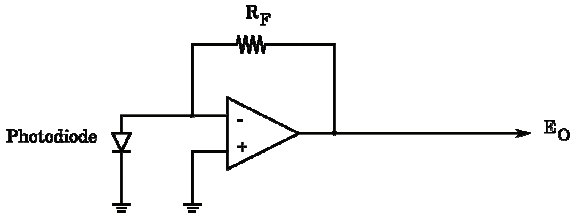

Figure 2: Transimpedance amplifier.

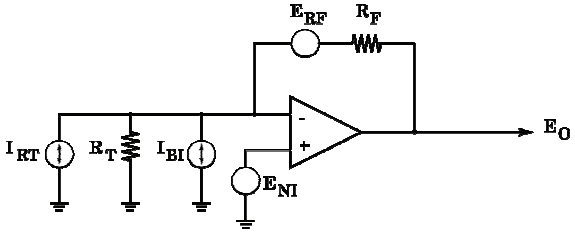

Figure 3: TIA with noise terms.

Including a term for the ADC noise voltage, ΔV_{ADC}, and the voltage reference noise, ΔV_{REF}, in Eq. 3 we find a noise model for the TIA:

$$E_O = \sqrt{(E_{NI}G_N)^2 + (I_{BI}R_F)^2 + 4kTR_FG_N + \Delta V_{ADC}^2/N + \Delta V_{REF}^2}\ , \quad (4)$$

where typically N = 250 ADC samples are averaged per data point. We calculate the SNR of the noise model using the expression

$$SNR = 10\log_{10}(I_{PC}R_F / E_O), \quad (5)$$

where I_{PC} is the photocurrent. One multiplies the logarithm in Eq. 5 by 10 instead of 20 when calculating the SNR because the photocurrent is proportional to the luminosity of light arriving at the photodiode and luminosity is luminous power per unit area.

A plot of the noise model, Figure 4, has three straight segments and a different term from Eq. 4 is dominant in each segment. The left segment has a slope proportional to $1/R_T$ and is due to the E_{NI} term in Eq. 4. As E_{NI} increases the left segment of the curve will shift down. The middle segment has a slope inversely proportional to the square root of R_T and is due to the third term, the thermal noise. An increase in thermal noise will reduce the SNR. The middle section of the curve also shows that increasing R_T increases the SNR. The final, flat section arises from the combination of noise from thermal noise of the feedback resistor, input current noise, ΔV_{ADC}, and ΔV_{REF}. Calculating these noise voltages with our final component values shows that the voltage reference noise provides the SNR limit within the right segment of Figure 4.

2.2.2 Photodiode

The IR photodiode I-V characteristic differs from typical Si photodiode characteristic curves in several ways. The IR photodiodes have lower reverse breakdown voltage, higher reverse saturation current, lower shunt resistance, and, when operating as part of the glucose sensor, lower photocurrent than Si photodiodes. For example the IR photodiodes have reverse breakdown of 1 to 2 volts and reverse saturation current of approximately 1μA. The S1133 has a maximum reverse voltage of 10V and dark current of 15 pA at 10V reverse voltage (Hamamatsu, 2001).

From our experimental results I_{PC} is measured to be 10 nA. We chose a value of 10 MΩ for R_F in order to yield a signal voltage of 0.1 V that is within the input range of the ADC. The relatively small photocurrent due to the limited amount of light reaching the filter and limited amount of light transmitted through the filter reduce the achievable SNR when compared to Si photodiodes in typical applications. For example, the S1133 Si photodiode can provide 100 μA of output current with high enough illumination (Hamamatsu, 2001), which is 10,000 times more photocurrent than we can obtain from our glucose sensor.

The IR photodiodes have shunt resistance, R_T, of approximately 30 kΩ. This also increases the difficulty in increasing SNR since the thermal noise is proportional to the amplifier gain, $1 + R_F/R_T$. The typical S1133 shunt resistance is 100 GΩ (Hamamatsu, 2001), much greater than the IR photodiode shunt resistance. The low shunt resistance is due to the increased bandgap wavelength of the IR photodiodes (2.5 μm) versus that of typical silicon diodes (1.1 μm).

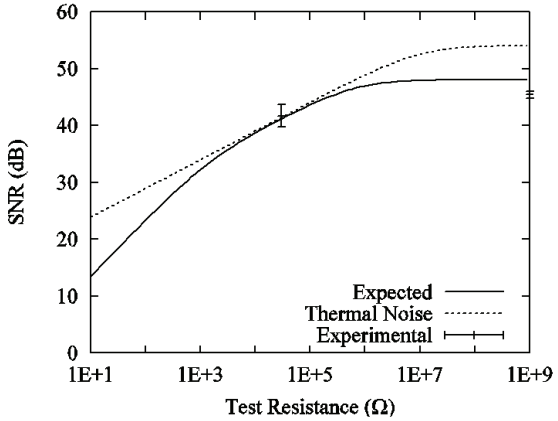

Figure 4: Plot of the output from our noise model with N=250. Thermal noise and experimental data also shown for comparison.

We cannot reverse bias the IR photodiodes due to their high reverse saturation current. Increasing reverse bias increases the dark current and shot noise on the dark current would dominate other noise sources and reduce the SNR. Also, since the dark current increases with more reverse bias as the photocurrent remains constant, a smaller portion of the current flowing into the TIA is due to the photocurrent, reducing the SNR.

2.3 Circuit Design

Figure 5 shows the final circuit design used for each channel. We added the shot noise on the offset current, op amp input current noise, and op amp voltage noise for a number of op amps to select an op amp for the TIA. Here the offset current is the sum of the op amp input offset current and the current in R_T due to the op amp offset voltage. We included shot noise on the offset current since the source of the photodiode current is a diode junction. We chose the MAX4478 (Maxim, 2005) because it minimized the sum of these noise voltages.

The chief factors affecting choice of the ADC are the resolution, number of delta-sigma (Δ-Σ) blocks in the device, ability to daisy-chain serial data ports of devices, and conversion time. We chose a 24-bit Δ-Σ ADC with 8 channels, 8 Δ-Σ blocks, and maximum sampling rate of 52.7 kHz when using high resolution (Texas Instruments, 2008). Four ADCs are necessary to sample all 32 channels simultaneously. We need a minimum of 20 bit ADC resolution to keep the quantization error well below the system noise. Since there is one Δ-Σ block for each photodiode channel, multiplexing ADCs is unnecessary, allowing time efficiency and simplifying the software required to archive data.

The serial ports of the ADC we chose can be daisy-chained which also simplifies the system because only one serial port is required. We need to record four types of samples to calculate the glucose concentration: with LED 1 on/LED2 off, both LEDs off, LED1 off/LED2 on, and both LEDs off. Since we sample all channels simultaneously and typically record N = 250 samples per second, recording four types of data samples requires a sampling rate of 1

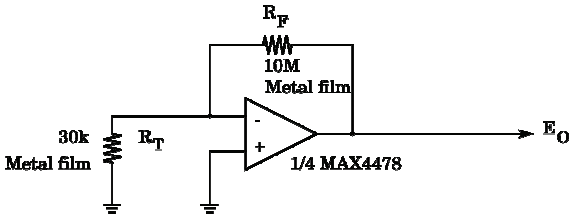

Figure 5: Schematic of one DAU channel.

kHz, well below the ADS1278 maximum sample rate. We selected a low noise voltage reference with noise voltage of 1.5 μV and a low temperature coefficient of 0.6 PPM/deg. C. (Cirrus Logic, 2009)

3 EXPERIMENT AND RESULTS

Figure 6 shows the method we use to record experimental data. The time per data point, T_{Data}, is 1 second and N = 250 so that T_{Sample} = 1/250 second. The DAU samples the voltage on all channels at points labeled S_n. At points labeled D_m the average value of the samples for all channels are calculated and archived. When we use the glucose sensor the four types of data mentioned above must be recorded in each sample period to calculate the glucose concentration. While verifying the SNR of the DAU system in this paper we utilize low noise resistors and only one of the four types of data is required since there are no LEDs present without the glucose sensor.

To test the SNR we record a large (1k data points) set of experimental data and calculate the SNR. Figure 7 shows a plot of channel voltage vs. time for a representative channel. Figure 7 shows 2000 data points from channel 1 taken at a rate of 1 Hz – the last 1000 data points were used to calculate the SNR. The plot shows approximately 20 μV of drift with +/- 10 μV of noise in the last 1000 data points. The standard deviation of this portion of data is 9.12 μV and the SNR for channel 1 is calculated to be 40.4 dB. Fig. 8 shows the SNR for all 32 channels. The mean SNR is 41.7 dB and the standard deviation of the SNR is 2.0 dB. Channels 15 and 31 do have 5 to 7 dB more noise than the other channels. This is likely due to slight differences in noise characteristics of the op amps. Fig. 4 also shows the thermal noise present in the

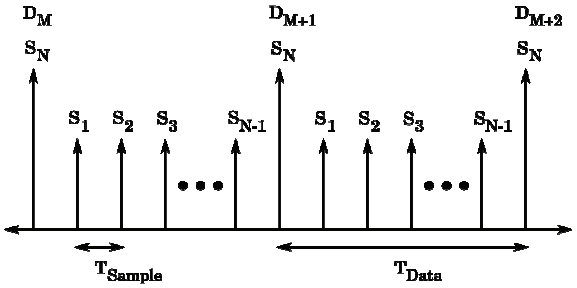

Figure 6: Method for recording experimental data. Channels are sampled at S_n and data points are calculated and recorded at D_m.

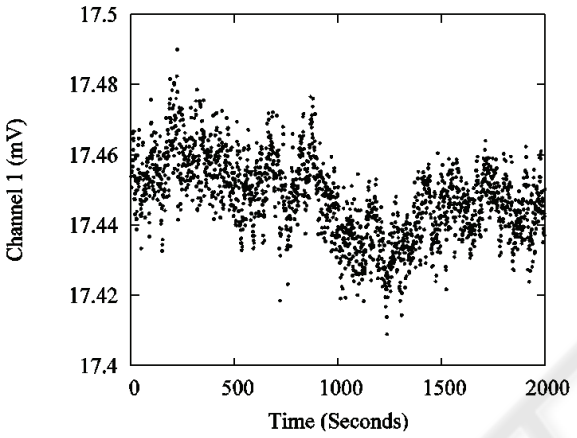

Figure 7: Voltage on channel 1 versus time.

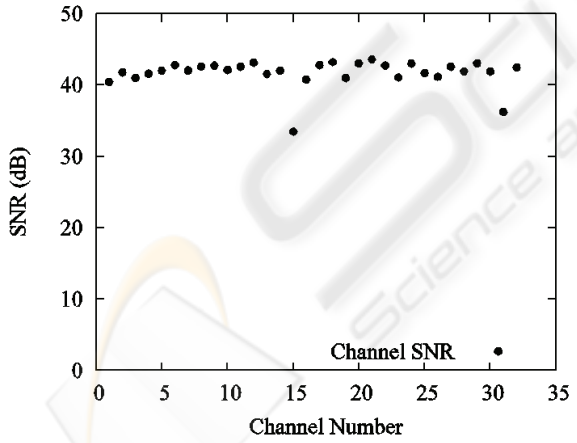

Figure 8: SNR of all 32 channels.

TIA to indicate the maximum SNR possible if the op amps, ADCs, and voltage reference were ideal components. The experimental results are within one standard deviation of both the expected noise and thermal noise for R_T = 30 kΩ but the experimental data point with an open circuit, 45.4 dB, is slightly below the expected noise of 48 dB. This difference has been traced to excess ripple on the voltage reference supply voltage.

4 DISCUSSION

Although thermal noise limits the DAU SNR when using low noise metal film test resistors, additional noise sources will be present when using actual glucose sensors with the DAU. The photocurrent and dark current would both provide shot noise since they originate from a diode junction. In order to eliminate shot noise from dark current the photodiodes cannot be reverse biased. The shot noise from 10 nA of photocurrent is 57 fA. The voltage created by this current passing through R_F is 0.57 μV. The mean SNR of 41.7 dB corresponds to 6.76 μV of noise voltage. Adding these two noise voltages still results in 41.7 dB SNR so the shot noise on the photocurrent will not significantly degrade the SNR.

A fan cooled the DAU to reduce the effects of thermal drift during our experiments. This is reasonable here since when the DAU and glucose sensor are designed into an implantable device the system will be in an environment with constant temperature.

5 CONCLUSIONS

The experimental measurements of SNR agree very well with the SNR calculated with the noise model for the TIA. The experimental SNR of 41.7 dB for R_T = 30 kΩ is also very close to the thermal noise limit, i.e., it is the maximum SNR possible with this TIA design and R_T of 30 kΩ. This indicates the DAU is acceptable for use with prototype glucose sensors and for future miniaturization of the DAU system and glucose sensor into a continuous glucose monitoring system.

A noise model was developed for the DAU and experimental data verified that the system works as expected by theory. In the future we will use the DAU to test glucose sensors by measuring absorption spectra of water and glucose. We also plan studies using ISF with the glucose sensors before miniaturization of the sensor and DAU electronics.

ACKNOWLEDGEMENTS

The authors would like to acknowledge support from NIH Grant No. DK064569.

REFERENCES

Olesburg, J. T., Cao, C., Yager, J. R., Prineas, J. P., Coretsopoulos, C., Arnold, M. A., L. J. Olafsen, L. J., Santilli, M., 2006. *Proc. of SPIE* **694**, 609403.

Centers for Disease Control and Prevention, 2007. *"National Diabetes Fact Sheet, 2007,"* Department of Health and Human Services - Centers for Disease Control and Prevention.

Saudek, C. D., Derr, R. L., Kalyani, R. R., 2006. *JAMA* **295** No. 14 p. 1688.

Chia, C. W., Saudek, C. D., 2004. *Endocrinol. Metab. Clin. N. Am.* **33** p. 175.

Rebrin, K., Steil, G. M., 2000. *Diabetes Tech. and Therapeutics* **2** No. 3 p. 461.

Motchenbacher, C. D., Connelly, J. A., 1993. *Low-Noise Electronic System Design*, John Wiley and Sons. New York.

Steffes, M., 2005. Application Report SBOA066A, *"Noise Analysis for High-Speed Op Amps,"* (www.ti.com).

Hamamatsu, 2001. Datasheet, "*Si Photodiode S1087/S1133 series*," Hamamatsu Photonics K. K.

Maxim, 2005. MAX4478 datasheet. *"MAX4478 SOT23, Low-Noise, Low-Distortion, Wide-Band, Rail-to-Rail Op Amps,"* Maxim Integrated Products, Inc.

Texas Instruments, 2008. ADS1278 datasheet. *"ADS1278 Quad/Octal, Simultaneous Sampling, 24-Bit Analog-to-Digital Converters,"* Texas Instruments, Inc.

Cirrus Logic, 2009. VRE3025 datasheet. *"VRE3025 Precision Voltage Reference,"* Cirrus Logic, Inc.